Nature of inclined growth in thin-layer electrodeposition under uniform magnetic fields

Alejandro Soba*
Centro Atómico Constituyentes, Comisión Nacional de Energía Atómica and Consejo Nacional de Investigaciones Científicas y Técnicas, Buenos Aires, Argentina

Graciela González
INQUIMAE - Departamento de Química Inorgánica, Analítica y Química Física, Facultad de Ciencias Exactas y Naturales, Universidad de Buenos Aires, and Consejo Nacional de Investigaciones Científicas y Técnicas, Buenos Aires, Argentina

Lucas Calivar
Laboratorio de Sistemas Complejos, Departamento de Computación, Facultad de Ciencias Exactas y Naturales, Universidad de Buenos Aires, Buenos Aires, Argentina

Guillermo Marshall†
Laboratorio de Sistemas Complejos, Departamento de Computación, Facultad de Ciencias Exactas y Naturales, Universidad de Buenos Aires, and Consejo Nacional de Investigaciones Científicas y Técnicas, Buenos Aires, Argentina
(Received 15 July 2012; published 30 November 2012)

Electrochemical deposition (ECD) in thin cells in a vertical position relative to gravity, subject to an external uniform magnetic field, yields a growth pattern formation with dense branched morphology with branches tilted in the direction of the magnetic force. We study the nature of the inclined growth through experiments and theory. Experiments in ECD, in the absence of magnetic forces, reveal that a branch grows by allowing fluid to penetrate its tip and to be ejected from the sides through a pair of symmetric vortices attached to the tip. The upper vortices zone defines an arch separating an inner zone ion depleted and an outer zone in a funnel-like form with a concentrated solution through which metal ions are carried into the tip. When a magnetic field is turned on, vortex symmetry is broken, one vortex becoming weaker than the other, inducing an inclination of the funnel. Consequently, particles entering the funnel give rise to branch growth tilted in the same direction. Theory predicts, in the absence of a magnetic force, funnel symmetry induced through symmetric vortices driven by electric and gravitational forces; when the magnetic force is on, it is composed with the pair of clockwise and counterclockwise vortices, reducing or amplifying one or the other. In turn, funnel tilting modifies particle trajectories, thus, growth orientation.

DOI: 10.1103/PhysRevE.86.051612 PACS number(s): 68.70.+w, 61.43.Hv, 82.20.Wt

I. INTRODUCTION

Electrochemical deposition (ECD) of ramified deposits in thin-layer cells gives rise to complex geometries, ranging from fractal to dense branch morphology, depending on cell geometry, its orientation relative to gravity, electrolyte concentration, cell voltage, and other parameters. The addition of a magnetic field also has strong effects on the ECD. From the morphogenesis perspective, the application of a weak external magnetic field perpendicular to the plane of the growth generates pattern spiraling and/or asymmetrical branching, for instance, in copper and zinc growths in aqueous solutions. In Refs. [1,2], examples of Zn deposits, grown under these conditions, are presented; there is a morphological tendency to form spirals with branches gyrating counterclockwise or clockwise, depending on the magnetic field direction. In some experiments, the main branches show some asymmetry as well, i.e., in which secondary branches at one side of the central nerve are longer than on the other [2]. In the literature on quasi-two-dimensional electrochemical deposition, two main groups of processes have been addressed: the first related to kinetic transfer, including chemical mechanisms as well as surface phenomena at the growing front and the second related to mass transport due to diffusion, migration, and convection. Convection here is mainly driven by electric, gravitational, and magnetic forces, hereafter, Coulomb, Archimedes, and Lorentz, respectively. Many papers in the literature show that no significant field effect due to kinetic transfer should be expected; on the contrary, many more papers evidence its influence on mass transport. Magnetohydrodynamics (MHD) convection [3,4] is a well-known effect due to the magnetic or Lorentz body force. This force induces ion motion and MHD flow by momentum transfer of these ions to the surrounding solvent [5,6] as illustrated in Ref. [2] where fluid motion is visualized by tracking optically opaque oil microdroplets added to the electrolyte. When a magnetic field is applied in the positive direction (z axis), a global fluid motion in counterclockwise rotation is observed. In brief, experience from these and other authors confirms the occurrence of MHD convection induced by the Lorentz force upon application of an external magnetic field [7]. This effect could be attenuated by increasing fluid viscosity [8]. A secondary effect, related to the MHD force, appears in the diffusion layer close to the electrode when the magnetic field applied is orthogonal to the current. Here, the Lorentz force, acting on local charges, induces a motion parallel to the interface (electrokinetic

*soba@cnea.gov.ar
†marshallg@arnet.com.ar

magnetohydrodynamics effect) [7,9]. This effect was analyzed in Ref. [10] where it was concluded that the magnetic field did not affect the kinetics of transference. Computational modeling has been successfully used in studying the nature of electrochemical deposition. Models, showing the deposit growth seen as a fractal growth with or without a magnetic field, were presented in Refs. [11,12]. They were based on the diffusion-limited aggregation (DLA) mechanism [13] to which the effect of migration, diffusion, and fluid convection was added [1,14–16]. In Refs. [1,14], morphologies observed in thin cell electrodeposition under a magnetic field normal to the cell were simulated with a DLA algorithm using a term representing fluid rotation. With this model, it was possible to reproduce the chirality induced by the magnetic field observed in the experiments. In other papers, models were based upon the introduction of the Coulomb forces, resulting from the electrostatic potential and the Lorentz forces induced by the magnetic field applied perpendicular to the plane of the cell [4,17]. All these models of electrodeposition under magnetic fields consider the deposit as a fractal growth and use a one-field equation to describe them. However, more realistic models need to take mass transport and deposit growth into account. The goal of this paper is to study the nature of inclined growth in thin-layer electrodeposition under uniform magnetic fields taking into account mass transport and deposit growth. In this context and considering that convection certainly increases ECD complexity and that it is natural to try to reduce its influence, in this paper, we analyze ECD in a cell in a vertical position relative to gravity and with the cathode above the anode as an example of the convection reduced ion transport regime. In this configuration, ECD gives rise to electrodeposits that are close to what is termed dense branch morphology, see, for instance, Ref. [18]. Also, they possess a uniform front rather than a hierarchy of branch sizes as seen in horizontal cells. Although global convection is suppressed, this configuration plays an important role in electrodeposition. The role of convection in ECD in thin cells in a vertical position relative to gravity with a cathode above an anode (without a magnetic field) was thoroughly analyzed in Refs. [19–23]. The role of convection in ECD in very thin cells (30 μm) in a horizontal position relative to gravity on the formation of meshlike electrodeposits is worth mentioning. This was specially studied in Refs. [24,25] where it was found that symmetry of the convective vortices on the two sides of the growing tip is responsible for whether or not a meshlike structure is formed. For describing ECD under a magnetic field (MECD), we introduce a phenomenological macroscopic model using first principles taking into account the most relevant variables of the problem and considering ion transport, electrostatic potential, and viscous fluid under electric, magnetic, and gravity forces. Its mathematical analogy includes the Nernst-Planck equations for ion transport, the Poisson equation for the electrostatic potential, the Navier-Stokes equations for the solvent, taking into account the Lorentz force represented by an external magnetic field, and a growth law based on a discrete version of a DLA presented in Refs. [4,17]. In order to validate the mathematical model, experimental results of MECD with and without magnetic fields are presented. Particle image velocimetry is used for showing the underlying flow pattern determining growth mechanism in MECD. The paper is divided as follows: Sec. II presents experimental measurements and a phenomenological model, Sec. III introduces a theoretical analysis of the ECD with a magnetic field, Sec. IV presents a general discussion, and Sec. V gives some conclusions.

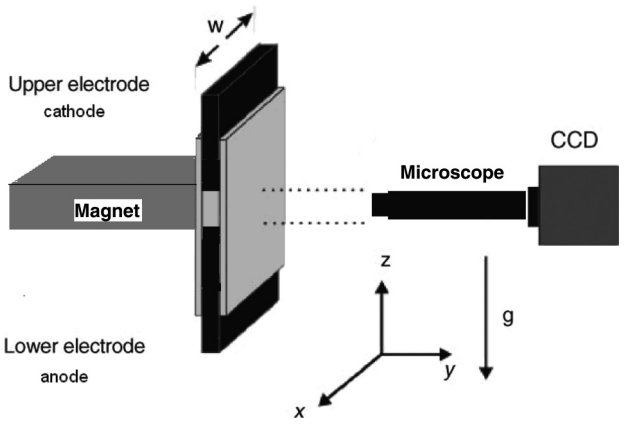

FIG. 1. Experimental setup.

II. EXPERIMENTAL RESULTS

All the experiments were carried out using a thin-layer cell in a vertical position relative to gravity, placing the cathode above the anode to attenuate convection. The cell consists of a thin layer of unsupported electrolyte solution confined between two parallel glass plates (see Fig. 1). The electrolyte solution was 0.1 mol/l $CuSO_4$. Copper plate electrodes were placed at both ends of the cell with a separation of $L = 5$ mm; their thickness of 0.127 mm defined the thickness d of the cell. The cell width was $w = 25$ mm. For fluid tracking, latex spheres with a diameter of 0.9 μm were added to the electrolyte, and lateral illumination was used to visualize particles by the Tyndall effect. Video images were digitized and were saved to disk at up to 10 frames/s with a spatial resolution of up to 3.5 μm/pixel. A public domain software package [26] was used for image capturing and processing. In some of the experiments, an artificial spike was used in an otherwise flat electrode to mimic a leading branch and its neighbors. In the experiments referred to as "with a magnetic field," a 1 T magnet was placed behind the cell covering the whole space between electrodes. The experiments were carried out under galvanostatic conditions at 2 mA.

With the aim of describing how Lorentz forces influence the hydrodynamic pattern and the growth in the thin-layer cell electrochemical deposition in a vertical position relative to gravity (cathode above anode), we need to recall the macroscopic phenomenological model for a cell in a vertical position in the absence of a magnetic field [21]. When the circuit is closed, current starts flowing through the cell, and ion concentration boundary layers develop near the electrodes. At the anode, the concentration is increased above its initial level due to the transport of anions from the cathode region and the dissolution of metal ions from the anode. At the cathode, the ion concentration is decreased as metal ions are reduced and are deposited out and anions drift away. These concentration variations lead to density variations and, therefore, to concentration fronts at the electrodes. In

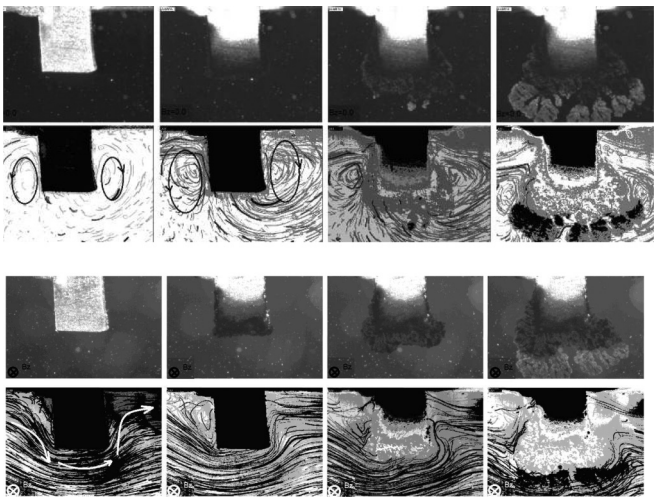

FIG. 2. Zoomed images of local growth and flow near a 1 mm × 0.5 mm artificial spike at 5, 20, 40, and 60 s during ECD with and without a magnetic field applied. Here, flow is visualized with tracking particles. The first two rows are without a magnetic field, and the last two are with a magnetic field applied normal to the plane of the growth and pointing away from the reader (positive sign).

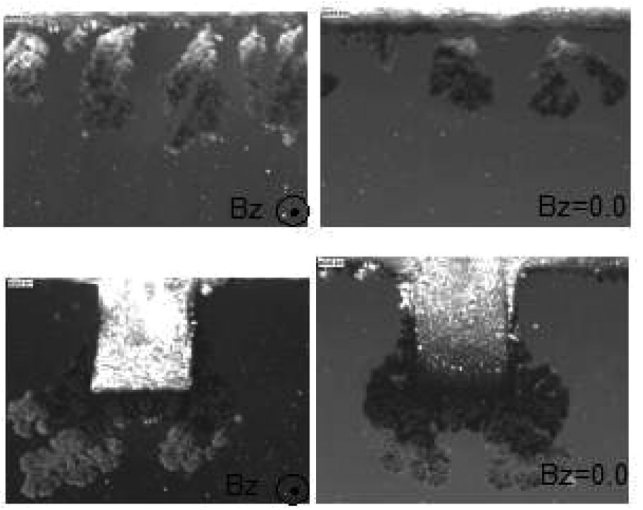

FIG. 3. Global growth at the cathode and zoomed local growth near a spike during ECD in the presence and absence of a magnetic field. Left column: top image shows global growth at the cathode when the magnetic field, normal to the plane of the growth, points towards the reader (negative sign); bottom image shows local growth near the spike under the same conditions. Right column: the same as in the left column but without a magnetic field.

this configuration, the high density fluid is below the low density fluid, hence, a stable stratified flow emerges in which gravitoconvection is suppressed. Stratification remains stable as long as there is no growth of branches. During this initial period, ion transport is mainly diffusive and migratory, and cation depletion at the cathode is uniform. Consequently, in a very narrow region near the cathode, a local uniform charge develops, giving rise to local Coulomb forces initially pointing towards the cathode. After a few seconds, instability develops, triggering the growth of a deposit at the cathode. Coulomb forces concentrate at the tips; each porous filament allows fluid to penetrate its tip and to be ejected from the sides, forming a vortex ring driven by the electric force. This is the mechanism by which branches grow. Clearly, the upper zone of the vortices defines a line in the form of an arch joining two adjacent tips. These arches define, between adjacent tips, an inner vortex zone ion depleted and an outer zone in a funnel-like form with a concentrated solution. The metal ions are carried into the tip of the branch through this funnel [27]. But, as soon as branches appear, stratification breaks down because the fluid concentration surrounding a downward growing branch tip diminishes, creating a concentration gradient and, thus, a local convection due to Archimedes forces. Therefore, at the branch tip, local convection is due to electric and gravitational forces. Since gravitational forces are normal to the growth, vortex symmetry and the induced funnel maintain symmetry [28]. To illustrate previous contentions, in Fig. 2, the first two rows of images show the local flow and growth, respectively, near a 1 mm × 0.5 mm artificial spike on an otherwise flat cathode during ECD. Here, flow, visualized with tracking particles, reveals that the vortex pattern is almost symmetrical and growth is symmetrical.

Following the macroscopic phenomenological model above, when a magnetic field is added to ECD, Lorentz forces are composed with Coulomb and Archimedes forces and impact on the fluid flow pattern and growth. Symmetry is broken, and growth and fluid are notoriously affected as illustrated in the last two rows of Fig. 2: Growth and fluid trajectories bend to one side. The effect is so strong, to the point that velocity direction changes according to the Lorentz force direction, and vortices are strongly attenuated. Obviously, since Coulomb and Archimedes forces are kept invariant, the bending is caused solely by the Lorentz forces. The underlying principle governing this process can be observed in the last row's first two images in Fig. 2, and its explanation can be advanced as follows. The clockwise magnetic field (positive sign) is composed with the pair of counterclockwise and clockwise vortices, respectively, in such a way that the left vortex (negative) is weakened and the right vortex (positive) is strengthened. This vortex imbalance induces an inclination of the funnel, now bending towards the right. As a consequence, particles entering into the funnel inclined to the right give rise to a branch inclined in the same direction. This is clearly seen in Fig. 2 in the third and fourth rows and column growths, respectively. We would like to remark that the vortex imbalance previously described is so large due to the strength of the Lorentz forces that the left vortex is washed away, although remarkably, growth is weakly inhibited (last row images in Fig. 2).

To further illustrate the effects of a magnetic force on growth and flow, Fig. 3 shows a global growth at the cathode and local growth near a spike in the presence and absence of a magnetic field. Left column: image at the top shows global growth at the cathode when the magnetic field, normal to the plane of the growth, points towards the reader (negative sign); the bottom image shows local growth near the spike under the same conditions. Right column: the same as in the left column but without a magnetic field. Again, in the absence of a magnetic field, the deposit growth tends to be symmetric and, when a magnetic field is on, bends.

To summarize, the underlying flow pattern, determining the growth mechanism in ECD, is substantially altered in the

presence of a magnetic field. In particular, vortex symmetry is broken, and this seems to be the principal source of branch tilt. In passing, it is interesting to note that, in the absence of magnetic forces, in the first instant after the circuit is closed and before any growth is observed, the existence of an almost symmetric pair of vortices near the spike is unveiled. This pair of vortices is the signature of the sudden appearance of electric and gravitational forces, the former due to electrode shape.

III. THEORETICAL FRAMEWORK AND NUMERICAL MODEL

The phenomenological model describes the diffusive, migratory, and convective motions of ions in a fluid subject to an electric and external magnetic field. The mathematical model consists of the Nernst-Plank equations for the concentrations of the copper ions, the Poisson equation for the electrostatic potential, and the Navier-Stokes equation for the solvent. These equations are written as

$$\frac{\partial C_i}{\partial t} = -\nabla \cdot \mathbf{j}_i, \tag{1}$$

$$\mathbf{j}_i = -\mu_i C_i \nabla\phi - D_i \nabla C_i + C_i \mathbf{v}, \tag{2}$$

$$\nabla^2\phi = -\frac{F}{\epsilon}(z_c C - z_a A), \tag{3}$$

$$\frac{\partial \mathbf{v}}{\partial t} + \mathbf{v}\cdot\nabla\mathbf{v} = -\frac{1}{\rho}\nabla P + \nu\nabla^2\mathbf{v} + \frac{\mathbf{f}_e}{\rho} + \frac{\mathbf{f}_g}{\rho} + \frac{\mathbf{f}_B}{\rho}, \tag{4}$$

$$\nabla \cdot \mathbf{v} = 0, \tag{5}$$

where F is the Faraday constant, ϕ is the electrostatic potential, C_i and $\mathbf{j}_i$ are the concentration and flux of the ionic species i, P is the pressure, and $\mathbf{v}$ is the velocity. ρ and ν are the density and viscosity of the medium, respectively; z_i, μ_i, and D_i, respectively, are the charge number, the mobility, and the diffusion coefficient of the species i; e is the electron charge, and ϵ is the permittivity of the medium. $\mathbf{f}_e = eE\sum_i z_i C_i$ represents the electric or Columbic force, $\mathbf{f}_g = \rho g$ is the buoyant or Archimedes force, and $\mathbf{f}_B = e\sum_i z_i C_i(\mathbf{v}_i \times \mathbf{B})$ is the magnetic or Lorentz force [2,21,29]. Here, we do not consider the contribution due to the presence of charged particles moving into a magnetic field and that of paramagnetic particles [9]. Systems (1)–(5), with appropriate initial and boundary conditions, are valid in a space-time domain defined by $G = [\Omega(t) \times (0,t)]$, where Ω is a three-dimensional region with boundary $\Gamma(t)$; this boundary moves according to a growth law based on a DLA algorithm taken from Refs. [2,4]. This algorithm moves the ions towards the minimum potential energy. Thus, the electric and Lorentz forces are introduced in a Metropolis algorithm variation. A random point nearby the particle is chosen, and the step to this new position is proportional to $\exp(-K\,du)$, where K is inversely proportional to temperature and du is the variation in energy between the new and the present positions. The net effect is to drive the particle towards the resultant force; du includes the Coulomb potential energy and the Lorentz term, but the algorithm may, at least in principle, be used with any other forces [4]. To calculate the Coulomb term, the algorithm takes the potential energy between the incoming particle and every position in the aggregation into account. Considering the aggregation as a sum of particles, the total charge of the aggregation is the sum of them multiplied by the individual charges Q. Then,

$$U_{\text{Coulomb}}(\mathbf{r}_i) = -q_i Q \sum_{k=1,N} \frac{1}{|\mathbf{r}_i - \mathbf{r}_k|}, \tag{6}$$

where U_{Coulomb} is the contribution to the potential energy of the Coulomb term. To include the voltage dependence between electrodes, we use $Q = CV$, where C is the capacitance between electrodes. In this model, both electrodes are considered to be far away from each other, i.e., the electric field between the electrodes is well known. The Lorentz term can be introduced using the form of the force between a charged particle and a magnetic field B applied perpendicular to the plane of the movement of that particle,

$$U_{\text{Lorentz}} = -q_i(\mathbf{v} \times \mathbf{B}) \cdot \mathbf{r}. \tag{7}$$

In this model, the only parameters are V, B, and K; their units are volts, teslas, and J^{-1} (inverse joules). For our simulations, K is fixed, thus, not taking into account temperature variation. Using the identity $\nabla \times (\nabla \times \Psi) = \nabla(\nabla \cdot \Psi) - \nabla^2\Psi$, the systems (1)–(5) are written in transport-vorticity form in terms of the vorticity ($\Omega = \nabla \times \boldsymbol{v}$) and stream function ($\mathbf{v} = \nabla \times \Psi$). The three-dimensional model is treated as a set of two two-dimensional models (as in Refs. [15,30,31]): one in the z-x plane (the plane of the growth) and one in the z-y plane (the plane normal to the plane of the growth). These models take the cell position relative to gravity into account. Here, we focus on the z-x model in accordance with previous experimental papers. The computational model solves systems (1)–(5), written in transport-vorticity form for (equal spacing in both directions) using finite differences and deterministic relaxation techniques. This solution is obtained through the system of difference equations similar to those presented in Refs. [15,20,31]. The resulting solution is then used to advance the interface with the DLA model previously discussed.

IV. RESULTS AND DISCUSSION

Below, we present numerical results with the aim of mimicking early stages in the experimental results shown in Figs. 2 and 3 and for supporting the macroscopic phenomenological model introduced earlier. The relative importance of Coulomb and Lorentz forces in the ECD process is studied varying the magnitude and orientation of the magnetic field while keeping constant Coulomb forces.

Figure 4 presents the simulated stream function contours and electric field (arrows) in a zoomed zone near a fixed spike in the first instants of the experiment. Figure 4(a), revealing the existence of a symmetric pair of vortices near the spike driven by Coulomb and Archimedes forces, corresponds to a null magnetic field. Figure 4(b), revealing a broken symmetry in the vortex pair, corresponds to the case where a magnetic field points towards the reader (negative sign). The counterclockwise magnetic field is composed with the pair of counterclockwise and clockwise vortices in such a way that the left vortex is strengthened and the right vortex is weakened. Figure 4(c) shows the inverse situation in which the right vortex is strengthened and the left vortex is weakened when the magnetic field is pointing away from the reader

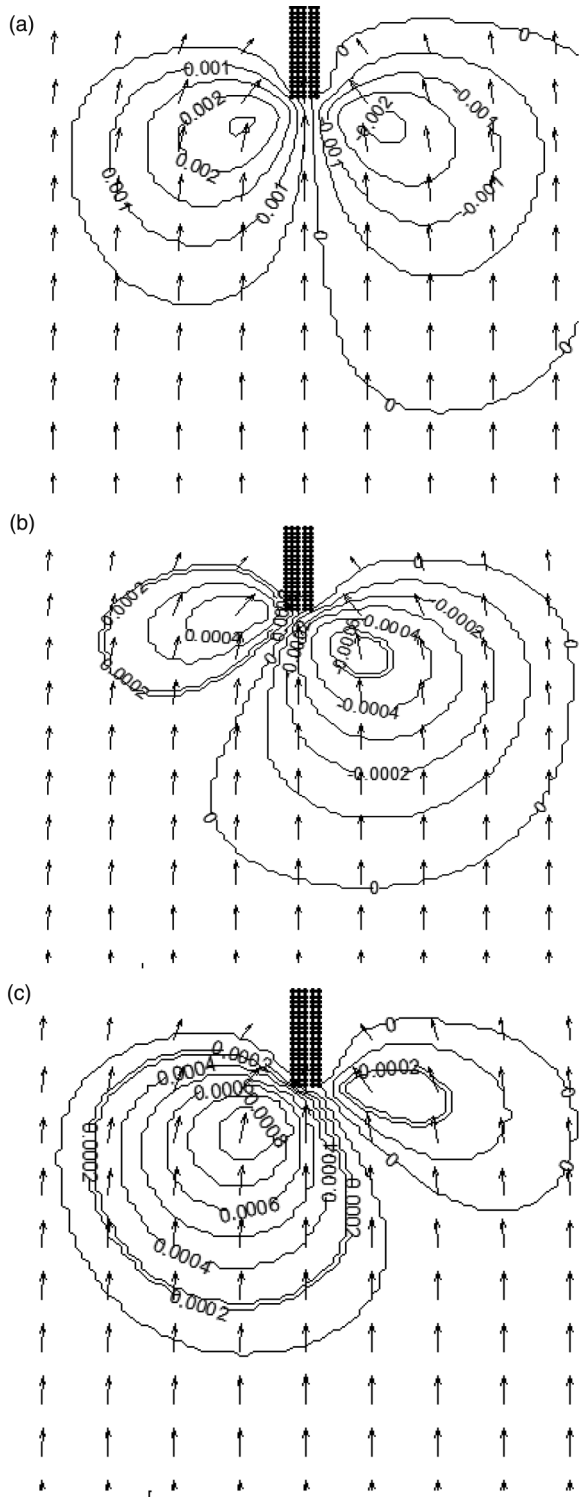

FIG. 4. Simulated stream function contours and electric field lines in a zoomed zone near the spike for (a) a null magnetic field, (b) a negative magnetic field, and (c) a positive magnetic field.

(positive sign). Clearly, the vortex pair strengthens to the left or right according to the magnetic force applied, following a similar pattern as that shown in the experiments. Although the electric field remains almost invariant under magnetic forces, concentration contour and the funnel-like form (just half of it shown) symmetry is again broken. In the range of

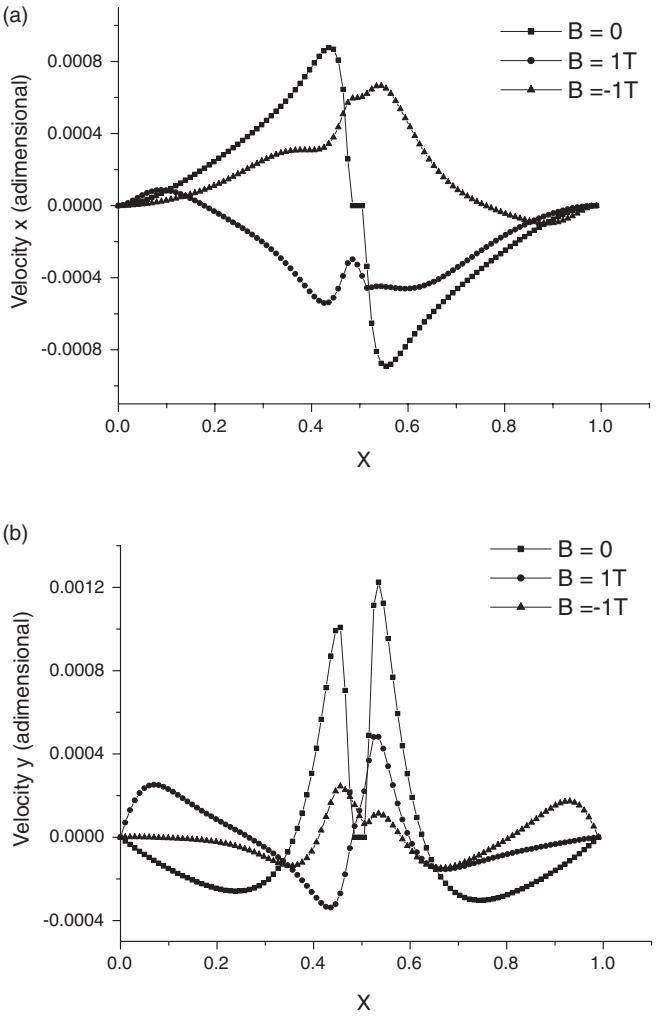

FIG. 5. (a) Variation in the x velocity component along the x axis when magnetic field B is zero, positive, and negative, respectively; (b) the same for the variation in the y velocity component.

parameters used in this simulation and at the beginning of the simulation, trajectories are less affected by the Lorentz forces than in the experiments described in Fig. 2; however, in the simulation, after a few seconds, vortices tend to disappear. Again, Lorentz forces are the sole cause of this phenomenon. Figure 5 presents the variation in the velocity components near the spike along a line parallel to the x axis when the magnetic force is null, positive, or negative, respectively. Figure 5 (top) shows the variation in the x velocity component along the x axis when the magnetic field B is zero, positive, and negative, respectively. Figure 5 (bottom) shows a similar graph for the variation in the y velocity component along the x axis. The x velocity component, when the magnetic field is null, shows the typical symmetry (with the sign changed) signature of the existence of a symmetric pair of vortices near the spike. The y velocity component is also almost symmetrical, although there is a sharp increase and decrease in the velocity in the center zone near the spike. In the presence of a magnetic field, both velocity components became positive or negative everywhere, according to the sign of the magnetic force,

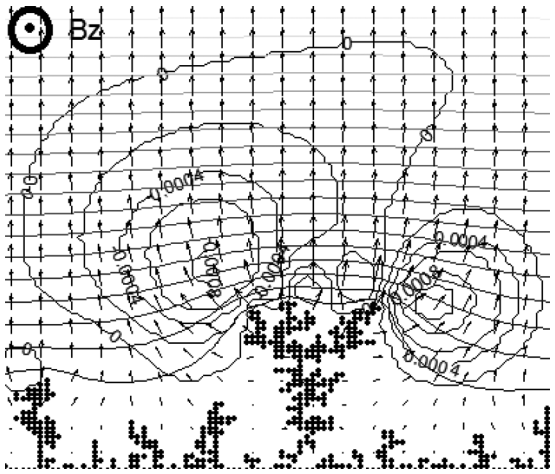

FIG. 6. Simulated stream function contours and arrows: electric field of an ECD experiment under a negative magnetic field (pointing to the reader) with a DLA growth law.

and their intensities were significantly reduced. This behavior follows a trend similar to that observed in the experiments. Having presented the three cases above, it is now possible to analyze the relative importance of Coulomb and Lorentz forces (Archimedes forces remain invariant). Clearly, when the magnetic field is null, the Coulomb force is at its maximum, and when a magnetic field is gradually applied, the relative importance of the Coulomb force decreases up to a point in which the Lorentz force becomes dominant as experimentally observed.

To pursue this analysis further, we need to introduce the simulation of the effect of a magnetic field in ECD with inclined fixed spikes (with an angle of inclination mimicking real experiments). This angle is zero if there is no magnetic field or a positive or negative magnetic field according to the sign of a nonzero magnetic field. The experiments with particles described in Fig. 2 show that the magnetic field is strong enough to very rapidly wash the vortex pair around the spike. Unfortunately, it was not possible to experimentally record the initial stages of the process. However, in the simulations, it is possible to predict the genesis of vortex evolution and disappearance due to the magnetic force using a small time step. For this, we initiate the simulation with a null magnetic field and a symmetric vortex pair as in the case of ECD with the null magnetic field shown in Fig. 5. As we increase the magnetic field and depending on its sign, the left or right vortex starts growing, and, after several steps (not shown here), one of the vortices disappears and the other grows until it occupies the whole cell. Immediately above the spike, velocity seems to follow the negative or positive direction observed in the experiments. As expected, cation acceleration near the deposit follows the direction of the magnetic field and governs fluid flow. This orientation determines the orientation of the deposit to the right or to the left, depending on the field magnetic sign as theoretically demonstrated in Ref. [8].

To enhance realism, Fig. 6 presents a simulation of an ECD experiment under a magnetic field with a growth law based on the DLA algorithm previously discussed. Here, every 100 time steps, the DLA algorithm is activated, and the deposit is allowed to grow. We used a small time step for numerical stability, which allowed more realistic deposits. We observe how the stream function shows a pronounced asymmetry due to the magnetic field. In the same fashion, the electric field (with arrows) is weaker in the zone between the deposit and the cathode. This allows some kind of relaxation and stabilization of the numerical model, resulting from a significant deposit structure modification due to the growth law. As in previous examples, the stream function reveals its asymmetry. Concentration contour lines and the funnel-like form are notoriously inclined to the left, accordingly determining growth. Also, the electric field is weaker in the zone between the growth and the cathode due to the screening produced by the growing branches. The use of a DLA model allows deposits to grow in the direction of minimum energy, which more realistically reflects the presence of an external magnetic field.

V. CONCLUSION

We presented experimental measurements and a two-dimensional theoretical model of electrochemical deposition in thin-layer cells under a uniform magnetic field. The theoretical model described the diffusive, migratory, electro-, and magnetoconvective ion transports and their deposition in thin cells through the Nernst-Planck equations for ion transport, the Poisson equation for the electric field, and the Navier-Stokes equations for the laminar fluid flow. A DLA model was used to simulate the growth of the deposits. Experiments in ECD, in the absence of magnetic forces, revealed that a branch grew normal to the cathode by allowing fluid to penetrate its tip and to be ejected from the sides through a pair of symmetric vortices attached to the tip. When the magnetic field was turned on, a branch grew inclined, relative to the cathode, tilting to the left or the right, according to the magnetic field sign. Experiments conducted around an enlarged spike for different magnetic forces showed that particle trajectories for the null magnetic field consisted of an almost symmetric pair of vortices near the spike. When a magnetic force was applied, trajectories were dramatically affected, to the point that vortex symmetry broke down, one vortex becoming weaker than the other, until disappearing, washed away by the other. Since Coulomb and Archimedes forces were kept invariant, the bending was caused exclusively by Lorentz forces. Moreover, experiments showed that branch tilting did not affect the fanning and splitting of the tips. Theory predicted the existence of an electrically and gravitationally driven symmetric pair of vortices at the tips that interacted with magnetic forces closely resembling the driving mechanism of branch growth observed in experiments. To summarize, the underlying flow pattern, determining the growth mechanism in ECD, was substantially altered in the presence of a magnetic field. In particular, vortex symmetry was broken, and this seemed to be the principal source of branch tilt.

ACKNOWLEDGMENTS

This work was supported by grants from Universidad de Buenos Aires (Grant No. UBACyTX132/08), CONICET (Grant No. PIP112-200801-01087/09), and MINCyT (Grant No. SLO-AR 08/02/09).

[1] T. R. Ní Mhíocháin and J. M. D. Coey, Phys. Rev. E **69**, 061404 (2004).
[2] S. Bodea, R. Ballou, and P. Molho, Phys. Rev. E **69**, 021605 (2004).
[3] H. Haus and J. Melcher, *Electromagnetic Fields and Energy* (Prentice Hall, Englewood Cliffs, NJ, 1989).
[4] C. M. Cronemberger and L. C. Sampaio, Phys. Rev. E **73**, 041403 (2006).
[5] S. Nakabayashi, K. Inokuma, and A. Karantonis, Phys. Rev. E **59**, 6599 (1999).
[6] G. Hinds, F. E. Spada, J. M. D. Coey, T. R. Ní Mhíocháin, and M. E. G. Lyons, J. Phys. Chem. B **105**, 9487 (2001).
[7] C. O'Reilly, G. Hinds, and J. M. D. Coey, J. Electrochem. Soc. **148**, C674 (2001).
[8] P. Fricoteaux, B. Jonvel, and J.-P. Chopart, J. Phys. Chem. B **107**, 9459 (2003).
[9] N. Leventis, M. Chen, X. Gao, M. Canalas, and P. Zhang, J. Phys. Chem. B **102**, 3512 (1998).
[10] O. Devos, O. Aaboubi, J. P. Chopart, E. Merienne, A. Olivier, C. Gabrielli, and B. Tribollet, J. Phys. Chem. B **103**, 496 (1999).
[11] T. Vicsek, *Fractal Growth Phenomena* (World Scientific, Singapore, 1992).
[12] P. Meakin, *Fractals* (Cambridge University Press, Cambridge, UK, 1998).
[13] T. A. Witten and L. M. Sander, Phys. Rev. Lett. **47**, 1400 (1981).
[14] T. R. Ní Mhíocháin, G. Hinds, A. Martin, Z. Y. E. Chang, A. Lai, L. Costiner, and J. M. D. Coey, Electrochim. Acta **49**, 4813 (2004).
[15] G. Marshall and P. Mocskos, Phys. Rev. E **55**, 549 (1997).
[16] G. Marshall and E. Arguijo, Physica A **185**, 146 (1992).
[17] C. Cronemberger, L. C. Sampaio, A. P. Guimarães, and P. Molho, Phys. Rev. E **81**, 021403 (2010).
[18] M. Wang and N.-b. Ming, Phys. Rev. Lett. **71**, 113 (1993).
[19] G. González, A. Soba, G. Marshall, and F. Molina, Electrochim. Acta **53**, 133 (2007).
[20] G. González, G. Marshall, F. Molina, and S. Dengra, Phys. Rev. E **65**, 051607 (2002).
[21] E. E. Mocskos, G. González, F. Molina, and G. Marshall, J. Electroanal. Chem. **653**, 27 (2011).
[22] G. Marshall, E. Mocskos, G. González, S. Dengra, F. V. Molina, and C. Iemmi, Electrochim. Acta **51**, 3058 (2006).
[23] E. Mocskos and G. Marshall, Electron. Trans. Numer. Anal. **34**, 90 (2009).
[24] K.-Q. Zhang, M. Wang, S. Zhong, G.-X. Chen, and N.-b. Ming, Phys. Rev. E **61**, 5512 (2000).
[25] Y.-Y. Weng, B. Zhang, S.-J. Fu, M. Wang, R.-W. Peng, G.-B. Ma, D.-J. Shu, and N.-B. Ming, Phys. Rev. E **81**, 051607 (2010).
[26] *NIH image*, http://rsb.info.nih.gov (2011).
[27] V. Fleury, J. H. Kaufman, and D. B. Hibbert, Nature (London) **367**, 435 (1994).
[28] M. Wang, W. J. P. van Enckevort, N.-B. Ming, and P. Bennema, Nature (London) **367**, 438 (1994).
[29] L. D. Landau and E. M. Lifshitz, *Mecanica De Fluidos* (Butterworth-Heinemann, Oxford, 1987).
[30] G. Marshall, P. Mocskos, H. L. Swinney, and J. M. Huth, Phys. Rev. E **59**, 2157 (1999).
[31] G. González, G. Marshall, F. V. Molina, S. Dengra, and M. Rosso, J. Electrochem. Soc. **148**, c479 (2001).